Springer

Journal of
Mechanical
Science and
Technology

Journal of Mechanical Science and Technology 23 (2009) 2714~2721

www.springerlink.com/content/1738-494x
DOI 10.1007/s12206-009-0723-7

Prediction of fretting fatigue behavior under elastic-plastic conditions †

Ki Su Shin*

Department of Weapon Systems, Korea National Defense University, Seoul, 122-875, Korea

(Manuscript Received March 30, 2009; Revised June 12, 2009; Accepted June 15, 2009)

Abstract

Fretting fatigue generally leads to the degradation of the fatigue strength of a material due to cyclic micro-slip between two contacting materials. Fretting fatigue is regarded as an important issue in designing aerospace structures. While many studies have evaluated fretting fatigue behavior under elastic deformation conditions, few have focused on fretting fatigue behavior under elastic-plastic deformation conditions, especially the crack orientation and fatigue life prediction for Ti-6Al-4V. The primary goal of this study was to characterize the fretting fatigue crack initiation behavior in the presence of plasticity. Experimental tests were performed using pad configurations involving elastic-plastic deformations. To calculate stress distributions under elastic-plastic fretting fatigue conditions, FEA was also performed. Several parametric approaches were used to predict fretting fatigue life along with stress distribution resulting from FEA. However, those parameters using surface stresses were unable to establish an equivalence between elastic fretting fatigue data and elastic-plastic fretting fatigue data. Based on this observation, the critical distance methods, which are commonly used in notch analysis, were applied to the fretting fatigue problem. In conclusion, the effective strain range method when used in conjunction with the SMSSR parameter showed a good correlation of data points between the pad configurations involving elastic and elastic plastic deformations.

***Keywords*:** Elastic-plastic; Fretting fatigue; Finite element analysis; Critical distance method; Ti-6Al-4V

1. Introduction

Fretting fatigue occurs where the contacting surfaces of mechanical parts are subjected to normal pressure and oscillatory micro-slip. Stress distribution within the contact region is intensified due to the combination of contact stresses and remote loadings. The presence of increased stress fields in the contact area often promotes rapid crack initiation and accelerates crack propagation.

The subject of fretting fatigue is important for safety of a flight because fretting fatigue has been attributed to the failure of turbine engines. Specifically, fretting fatigue has been found to occur in dovetail joints between the turbine blade and turbine rotor interface, as seen in Fig. 1. The vibration of the turbine engine imposes cyclic loading on the rotor-to-blade interface joint and induces the conditions for fretting fatigue. Failure of this joint due to fretting fatigue cannot currently be predicted nor is there currently an accepted technique to account for fretting in the initial design. Therefore, designers must over-compensate for the potential of fretting by making these dovetail joints more robust than may actually be necessary. Yet, such over-compensation in the design of the joint leads to heavier, less efficient and more costly engines. Moreover, due to the inability to accurately predict failure caused by fretting fatigue, periodic maintenance inspections must be performed to ensure cracks do not propagate and lead to catastrophic failure. Such inspections increase maintenance time and cost.

Consequently, a number of studies have been performed to predict the behavior of fretting fatigue. Generally in fatigue analysis, crack nucleation and

† This paper was recommended for publication in revised form by Associate Editor Seong Beom Lee

*Corresponding author. Tel.: +82 2 300 2135, Fax.: +82 2 309 6233
E-mail address: ksshin@kndu.ac.kr

© KSME & Springer 2009

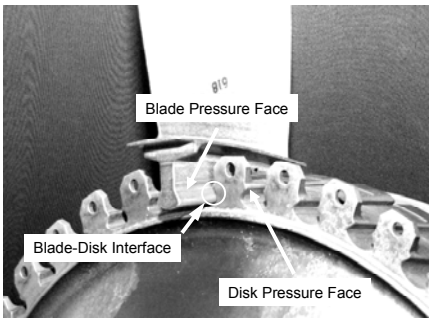

Fig. 1. Turbine engine dovetail joint.

propagation are characterized by parameters which are based on the state of cyclic stress, strain or any combination of these.

Generally, a large plastic zone is generated by the stresses, which exceed the material yield stress. In this situation, the stress gradient from the spot of peak stress is also very steep. Frequently, a high stress gradient is developed in notch problems especially from a sharp radius of the root tip. To account for the effect of stress concentration in the notch roots, various critical distance methods have been introduced.

One of the critical distance methods was the point method proposed by Peterson [1]. This method was based on the assumption that the failure occurs when the stress equals the fatigue strength at a constant distance beneath the notch tip for a given material. He related the quantity of K_f to K_t using the radius of the notch, r, and the material constant, a, as described below:

$$K_f = 1 + \frac{K_t - 1}{1 + \frac{a}{r}} \tag{1}$$

where K_t is the stress concentration factor, K_f is the fatigue notch factor.

Another well known averaging approach was the line method suggested by Neuber [2]. He formulated an equation that relates the stress concentration factor, K_t, into a fatigue notch factor, K_f, using a critical distance from the peak stress area. Both methods need critical distance that was assumed as a material property.

Since these critical distance parameters are very dependent on the test conditions and geometries, it is hard to generalize them for any other loading conditions and specimen geometries. Due to these restrictions on the application of critical distance, some researchers, such as Qylafku et al. [3] and Kadi [4], introduced a different approach called the volumetric approach, which did not include the fixed critical distance concept for each material. Instead of regarding the critical distance as material constants, they used the damage zone concept to find effective stress by investigating the stress gradient.

$$\sigma_{FI} = \frac{1}{V}\int_{\Omega} f\left(\sigma_{ij}\right)\varphi\left(\vec{r}\right)dv \tag{2}$$

where Ω is fatigue failure region and V is the volume of Ω. The fatigue failure region was assumed to be a circle or a sphere and its size was determined by the fitting of experimental results for each given material. The stress equivalent function, $f(\sigma_{ij})$, is von Mises equivalent stress for elastic-plastic stress distribution and $\varphi(\vec{r})$ is weight function. Using this approach, they demonstrated that the computed stress field intensity values are independent for the notched specimens and the specimens with key-seats.

Recently, Araujo and Nowell [5] calculated total fatigue lives analytically and compared them with experimental values under fretting fatigue conditions. From the analytical calculations using Smith-Watson-Topper (SWT) and Fatemi and Socie (FS) parameters, they demonstrated that the analytically calculated fatigue lives using surface stress distribution only was not adequate for predicting the fatigue lives, especially in the presence of a high stress gradient condition.

However, using the critical distance method and the volume method, which has a different approach to calculate the average stress, they successfully predicted the fretting fatigue lives. The formulations, i.e., SWT and FS, can be written as follows:

$$SWT = \sigma_{\max}\left(\frac{\Delta\varepsilon}{2}\right) \tag{3}$$

where $\Delta\varepsilon$ is the difference of the maximum and minimum strain and $\sigma_{\max}$ is the maximum value of the stress component during the cycle. The directions of both $\Delta\varepsilon$ and $\sigma_{\max}$ are perpendicular to the plane.

$$FS = \frac{\Delta\gamma}{2}\left(1 + \alpha\frac{\sigma_{\max}}{\sigma_y}\right) \tag{4}$$

where $\Delta\gamma$ is the difference of maximum and minimum values of shear strain experienced during the

cycle, σ_{max} is the maximum value of the stress normal to the chosen plane, σ_y is the yield strength, and α is a constant which approaches unity during long lives and is reduced during shorter lives.

Namjoshi et al. [6] also investigated the variation of critical plane parameters as changing the length of volume. By testing the SWT, FS and MSSR (modified shear stress range) parameters, they claimed that the MSSR parameter was the only parameter which can predict the behavior of the fretting fatigue reasonably.

$$MSSR = A\Delta\tau_{crit,effective}^{B} + C\sigma_{\max}^{D} \quad (5)$$

where the values of A, B, C, and D are determined as 0.75, 0.5, 0.75 and 0.5, respectively. In this parameter, the first term, $\Delta\tau_{crit,effective}$, is the same as the SSR [7] parameter, i.e., $\Delta\tau_{crit,effective} = \tau_{max}(1-R_r)^m$ where τ_{max} is the maximum shear stress on the critical plane, R_r is the shear stress ratio on the critical plane, and *m* is a fitting parameter. The second term is the maximum normal stress, σ_{max}, on the plane at maximum loading condition.

From the literature study noted above, it was found that a number of efforts have been made to analyze fretting fatigue. However, most studies were performed under the elastic condition, especially the crack initiation and fatigue life prediction for Ti-6Al-4V.

The objective of this proposed work is to expand on previous work in the area of fretting fatigue to the elastic-plastic condition using the averaging methods that have been used in notch problems. This study will involve both experiments and analyses.

2. Experiments

2.1 Material and specimen

Both the specimens and pads were machined from Ti-6Al-4V forged plates by the wire electrical discharge method. The longitudinal tensile properties (along the loading axis) were determined, i.e., the elastic modulus was 116 GPa and yield strength was 753 MPa. Fig. 2 shows schematics of the dog-bone specimen and the shapes of two different pad geometries. Table 1 shows the dimensions of all the pad geometries and normal load applied to the fretting pads.

2.2 Test setup and procedure

The fretting fatigue tests were conducted on a 22.2 kN servo-hydraulic uniaxial test machine at ambient temperature in a laboratory environment as shown in Fig. 3. This Fig. shows the rigidly mounted fretting fixture on a servo-hydraulic fatigue test machine used in this work.

Two load cells, one on each side of the specimen, were used to measure the normal load. A load cell, attached to the servo-hydraulic load frame on the top side of the specimen, measured the axial load above the pads. A lightweight pressure transducer was used to measure the axial load at the bottom of the specimen. This system allowed the user to vary the axial load by controlling the displacement in the axial direction. The displacement was applied in the axial direction at constant amplitude to allow the specimen to be adequately exposed to the prescribed loading conditions. The control system of the test equipment maintained the frequency and the amplitude of the applied axial displacement constant during the duration of the test. In this study, the displacement was applied in the axial direction at a frequency of 50 Hz.

Constant amplitude fretting fatigue tests were conducted over a wide range of applied axial force by

Table 1. Pad configurations and normal loads.

Pad name (mm)	R (mm)	Normal load (N)	Number of tested pads
Cyl. 50.8	50.8	1334	18
Cyl. 101.6	101.6	2224	15
Cyl. 304.8	304.8	4003	8
Cyl. 5.08 (1)	5.08	1334	16
Cyl. 5.08 (2)	5.08	1779	10

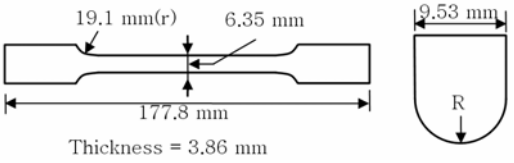

Fig. 2. Geometries of the specimen and fretting pads.

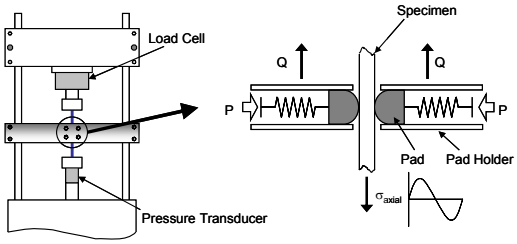

Fig. 3. Schematic of the fretting fatigue configuration.

servo-actuator on the bottom side of the specimen. The normal loads on the pads were applied with the aid of two lateral springs.

This load was held constant for the duration of the test and was monitored with a load cell. The normal loads were either 1334 N or 4003 N for each pad configuration as shown in Table 1. Higher normal loads were applied to generate the large plastic deformations. To perform finite element analysis (FEA), the axial and tangential loads must be determined, as each represents input data for FEA. As previously mentioned, a load cell was attached to the servo-hydraulic load frame on the top of the specimen to monitor the axial load. The tangential load can be determined by the equation:

$$Q = \frac{V - W}{2} \tag{6}$$

where Q is the tangential load on each side of the specimen, V is the axial load applied on the bottom side of the specimen, and W is the applied axial load on the top side of the specimen.

2.3 Test results

The prediction of crack location is one of the several measures of a predictive fatigue parameter; therefore, the crack location was determined for the each experimental test. Namjoshi et al. [6] evaluated fretting fatigue life of Ti-6Al-4V for the pad configurations involving elastic deformations: cylindrical pads with radii of 50.8 mm, 101.6 mm, 304.8 mm. They reported that the failure of all specimens with pad configuration involving elastic deformation occurred due to crack growth that initiated at the contact surface and near the trailing edge of contact. Similar results were found for the pad configurations involving elastic-plastic deformations included in this study: two 5.08 mm radius cylindrical pads with 1334 N and 1779 N normal loads. Fig. 4 shows scar from the 5.08 mm cylindrical pad with 1779 N normal load. As can be seen from figure, the crack initiation location was found near the trailing edge between specimens and pad configurations involving elastic-plastic deformations.

Crack initiation orientation was determined by mounting a sectioned specimen which had been made by grinding the specimen. Namjoshi et al. [6] reported that the experimentally observed primary crack orientations angles under elastic fretting conditions were

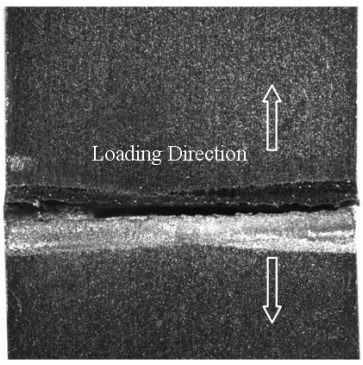

Fig. 4. Fretting scar from the 5.08 mm radius cylindrical pad.

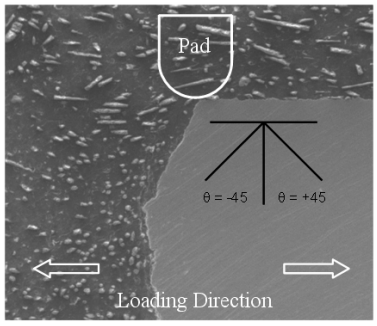

Fig. 5. Crack orientation of the 5.08 mm radius cylindrical pad.

either -45^0 or $+45^0$ with a variation of $\pm 15^0$ from a perpendicular to the loading direction. Fig. 5 shows the typical crack orientation of the 5.08 mm radius cylindrical pad with normal load 1,779 N. From the figure, it can be seen the crack orientation resulting from the pad configuration involving elastic-plastic deformation also has around –45° from a perpendicular to the loading direction.

3. Finite element analysis

3.1 Mesh modeling

4-node, plane strain elements were used in all three bodies of the finite element model: the fretted speci men, the fretting pad and fretting pad holder. 4-noded elements (bilinear) were chosen instead of 8-noded elements (serendipity), because the mid side node in the 8-noded element introduces an oscillation in the stress state along the contact surfaces as reported by Lykins et al. [8]. The contact between the pad and the specimen was defined by using the master-slave algorithm in ABAQUS for contact between two surfaces.

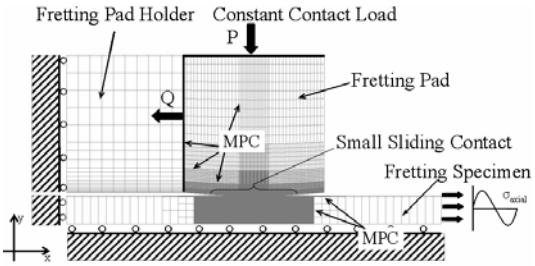

Fig. 6. Illustration of the typical finite element model mesh.

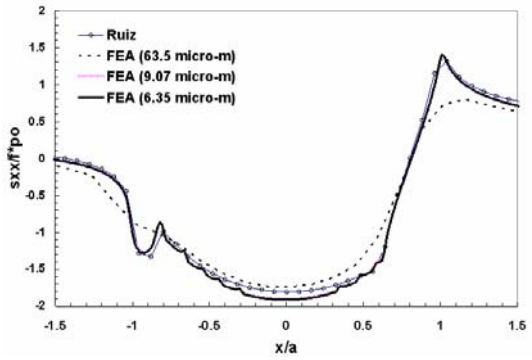

Fig. 7. The comparison of values σ_{xx} between Ruiz and FEA results.

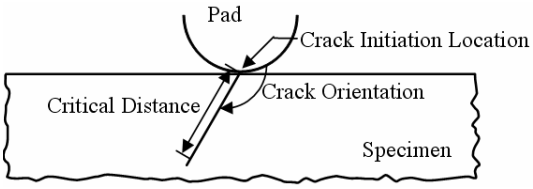

Fig. 8. Illustration of the critical distance along the critical plane.

The master surface is on the fretting pad and the slave surface is on the fretting fatigue specimen.

In this study, the FEA model used in Lykins [8] has been modified for the analysis of elastic-plastic fretting fatigue phenomenon. This FEA model has been refined for the purpose of analyzing local stresses and strains along and near the contact surface between pad and specimen.

Fig. 6 shows the mesh model of 50.8 mm radius cylindrical pad as an example. As seen in Fig. 6, the multi-point constraint (MPC) was applied at the top of the pad to prevent it from rotating due to the application of loads. The top nodes of the pad were forced to move in unison in the y-direction. Also, the MPC was applied to the boundary between regions where the mesh size of the elements differed. The MPC prevented the free nodes from penetrating the larger adjoining elements.

3.2 Verification of results

The mesh size within the fine mesh area was determined by comparison of the results between the FEA and analytical solutions. In this study, a FORTRAN program called "Ruiz," written by Chan and Lee [9], has been carried out as an analytical solution for the fretting fatigue condition. Since the analytical solution was based on the elastic condition, the FEA was performed with the elastic solution also. The 50.8 mm cylindrical pad configuration was selected for the comparison between FEA and analytical results. The following loading conditions were used for the verification of the proper mesh size: normal load, P = 1.33 kN, tangential load, Q = 0.3 kN, axial stress, axial = 55.2 MPa, coefficient of friction, COF = 0.5.

Fig. 7 shows the results of the comparison between the normalized σ_{xx} from the Ruiz program and the FEA calculation for the varied mesh sizes of the 50.8 mm cylindrical pad. As seen in this figure, the agreement between FEA and Ruiz calculations was improved as the mesh size decreased. For the square mesh with 6.35 μm for each side, the predicted contact half width, a, varied by 1.87% between FEA and Ruiz results, where a_{FEA} = 444 μm and a_{Ruiz} = 453 μm. The maximum pressure, P_o, predicted by the FEA model also agreed with the Ruiz program with a 0.4% difference; $P_{o\text{-}FEA}$ = 296.49 MPa versus $P_{o\text{-}Ruiz}$ = 295.3 MPa. The normalized maximum value of the longitudinal normal stress, σ_{xx}, varied by 6.1% between FEA and Ruiz results, where $\sigma_{xx\text{-}FEA}$ = 1.42 MPa and $\sigma_{xx\text{-}Ruiz}$ = 1.32 MPa. Therefore, in this study, the same mesh sizes were utilized for all pad geometries.

4. Analyses of fretting fatigue

4.1 Effective strain range method

In general, the strain-fatigue life approach has been commonly used for the elastic-plastic fatigue problem due to its capability to measure the large plastic deformation effects on fatigue life. In this study, the effective strain range, $\Delta\varepsilon_{effective}$, approach has been suggested as one method of finding effective critical distances, dc, under the fretting fatigue condition. Fig.

8 illustrates the crack initiation location, orientation and critical plane.

The formula of the effective strain, $\varepsilon_{effective}$, can be written as follows:

$$\varepsilon_{effective} = \frac{\sqrt{(\varepsilon_1-\varepsilon_2)^2+(\varepsilon_2-\varepsilon_3)^2+(\varepsilon_3-\varepsilon_1)^2}}{\sqrt{2}(1+\upsilon)} \quad (7)$$

The crack initiation locations were determined by the maximum value of $\Delta\varepsilon_{effective}$ on the contact surface. This effective strain range criterion predicts the crack initiation location at the contact surface and near the trailing edge of contact. This is in agreement with the observation from experimental work.

Fig. 9 shows the coordination of the stress state near the contact surface. Fig. 10 illustrates the effective strain for the tested pad configurations, i.e., the 50.0 mm radius cylindrical pad case. The figure is plotted by using the normalized total effective strain, ε_e, values by yield strain, ε_Y, value.

As mentioned before, the experimentally observed

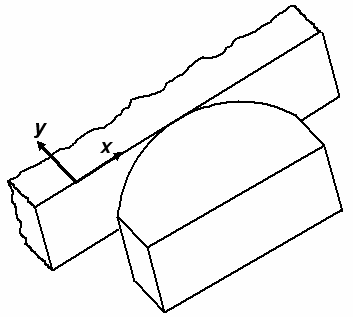

Fig. 9. The coordination of the stress state near the contact surface.

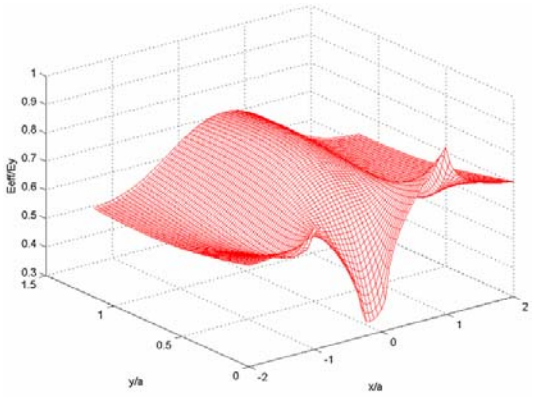

Fig. 10. $\varepsilon_{effective}$ near the contact surface for the 50.8 mm radius cylindrical pad.

primary crack orientations angles were either –45° or 45° with a variation of ±15° from the perpendicular to the direction of the applied loading. For this reason, -45° has been used for the crack orientation. The effective critical distance was determined at the location of a minimum value of $\Delta\varepsilon_{effective}$ along the critical plane. To find the effective critical distance, the first and second derivatives of the effective strain range curves were calculated to find the minimum value.

4.2 Result of the effective strain range method

Fig. 11 shows the results of the effective critical distances determined by the effective strain range method.

The effective critical distances have been determined by the distance from the crack initiation location to the point where the minimum value of effective strain range, $\Delta\varepsilon_{effective}$, occurs along the critical plane. The result shows increased effective critical distances as the number of cycles to failure increases.

For the cylindrical pads involving elastic deformations (cylindrical pads with radii of 50.8 mm, 101.6 mm and 304.8 mm), the effective critical distances

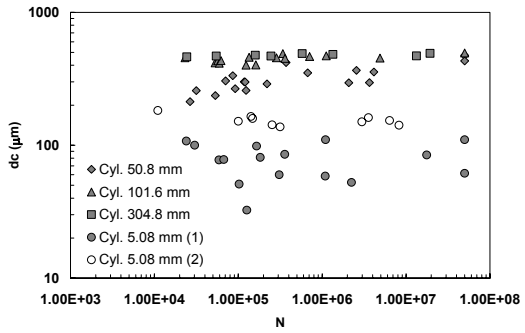

Fig. 11. Effective critical distances using effective strain range method.

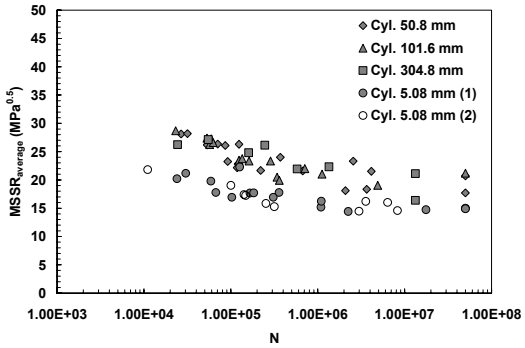

Fig. 12. The average MSSR values at dc=Min$\Delta\varepsilon_{effective}$.

decreased as the Hertzian peak pressure increased. Also, the effective critical distances were decreased as the number of cycle to failure decreased.

The small difference in the effective critical distances between cylindrical pads can be found in the high cycle fatigue regime. This is because cylindrical pads with radii of 50.8 mm and 101.6 mm have more increase of effective critical distances than that in the 304.8 mm radius cylindrical pad cases as the number of cycles to failure increases. The cylindrical pad configurations involving elastic-plastic deformations (two 5.08 mm radius cylindrical pads with different loading conditions) have shorter critical distance than the cylindrical pad configurations involving elastic deformations (three cylindrical pads with radii of 50.8 mm, 101.6 mm and 304.8 mm). This is because two 5.08 mm radius cylindrical pads have higher Hertzian peak pressure than do cylindrical pad configurations involving elastic deformations.

4.3 Results of the MSSR parameter

Fig. 12 shows the result of the MSSR parameter using critical distances determined by the effective strain range method in Fig. 11. The MSSR values were calculated from average stresses up to the given effective critical distances on the critical plane. However, the result of the MSSR parameter by the effective strain method is dependent on the pad configurations involving elastic and elastic-plastic deformations, and therefore the equivalence between elastic and elastic plastic deformation was not established.

Fig. 13 shows the end point values of the MSSR using the same effective critical distances. The end point values of the MSSR show wider scatter band in comparison to the result from average MSSR values as shown in Fig. 12. The distance between layered data points resulting from the pad configurations involving elastic deformation (cylindrical pads with radii of 50.8 mm, 101.6 mm and 304.8 mm) and elastic-plastic deformation (two 5.08 mm radius cylindrical pads) is enlarged, thereby increasing the overall scatter band.

4.4 Results of the SMSSR parameter

In this study, SMSSR (secondly modified shear stress range) parameter has been suggested to predict fatigue life under the fretting fatigue condition. The SMSSR parameter is expressed by the following formulation:

$$SMSSR = A\Delta\tau^{B}_{crit,effective} + C\Delta\sigma^{D}_{normal} \tag{8}$$

where $\Delta\tau_{crit,effetive} = \tau_{max}(1-R\tau)^{m}$, τ_{max} is the maximum shear stress on the critical plane, R_τ is the shear stress ratio on the critical plane, m is a curve fitting parameter determined to be 0.45 for Ti-6Al-4V, $\Delta\sigma_{normal}$ is the normal stress range on the critical plane where $\Delta\sigma_{normal}$ = abs (σ_{max}-σ_{min}), and A, B, C, D are curve fitting parameters determined to be 0.75, 0.5, 0.75, and 0.5 respectively for Ti-6Al-4V by Namjoshi et al. [6].

In the SMSSR parameter, the normal stress range,

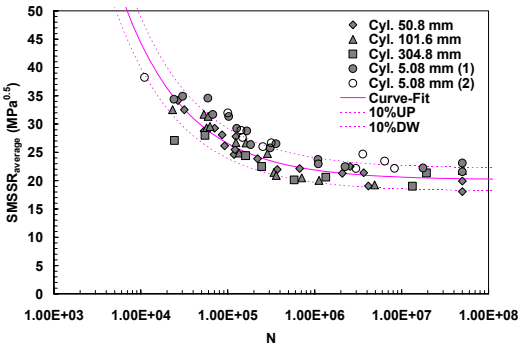

Fig. 14. The average SMSSR values at dc=Min$\Delta\varepsilon_{effective}$.

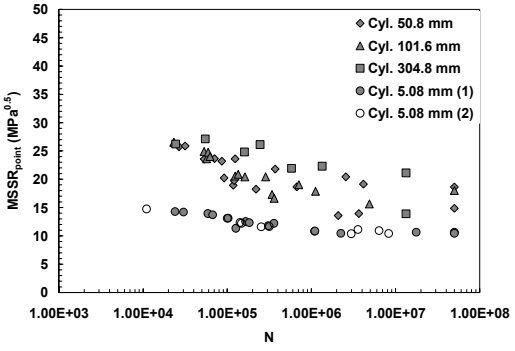

Fig. 13. The end point MSSR values at dc=Min$\Delta\varepsilon_{effective}$.

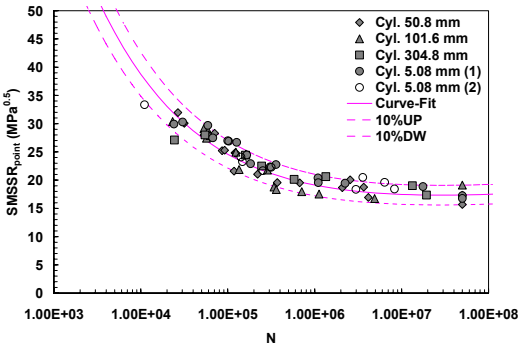

Fig. 15. The end point SMSSR values at dc=Min$\Delta\varepsilon_{effective}$.

$\Delta\sigma_{normal}$, values have been used instead of the normal stress amplitude, σ_{max}, in the MSSR parameter. This was done to account for the effects of the normal load on the critical plane at both maximum and minimum applied loading conditions.

Fig. 14 shows the data points of the SMSSR parameter using the effective critical distances, as shown in Fig. 11. These SMSSR values were calculated by using average stresses up to the effective critical distance. The curve-fitted line, which can be determined from data points, is also plotted in the figure. To measure the scatter band, the 10% upper and lower error line are also illustrated in the figure. Both the curve fit data and fretting fatigue data lie in a narrow scatter band with a mean error of 1.09 % and a standard deviation of 10.49. In the figure, the cylindrical pads show a good correlation of data points between the pad configurations involving elastic and elastic plastic deformations.

Fig. 15 shows end point values of the SMSSR parameters using the same critical distance. The results also show equivalence between the elastic and elastic-plastic fretting fatigue data. By comparing the end point values of the SMSSR to the averaged result of the same parameter in Fig. 14, it can be seen that the mean error decreased from 1.09% to 0.69%. Also, most of the data points fall within the narrow scatter range by 10% error.

5. Conclusions

Establishing an equivalence among fretting fatigue life data obtained from different pad geometries is always desirable since it eliminates or reduces the fretting fatigue experiments, which are significantly time consuming and relatively expensive to conduct.

In this study, two different parameters, MSSR and SMSSR, were utilized by using contact surface stresses to determine its potential as a fretting fatigue parameter. To account for the stress gradient near the contact surface, the critical distances approach commonly used in notch problems are introduced.

As a result, the effective strain range method when used in conjunction with the SMSSR parameter demonstrated as an approach that can predict the fretting fatigue life for both elastic and elastic-plastic conditions.

References

[1] Peterson, R. E, *Metal Fatigue*, McGraw-Hill, New York, USA. (1959) 293-306.

[2] Neuber, Heinz, *Theory of Notch Stresses: Principles for Exact Stress Calculation*, Ann Arbor, Michigan: J. W. Edwards (1949).

[3] G. Qylafku, Z. Azari, N. Kadi, M. Gjonaj and G. Pluvinage, Application of a new model proposal for fatigue life prediction on notches and key-seats, *International Journal of Fatigue*, 21: (1999) 753-760.

[4] Kadi N, Notch effect in high cycle fatigue, *NATO Sciences Series II, Kluwer*, (2001) 207-220.

[5] J. A. Araujo, D. Nowell, The effect of rapidly varying contact stress fields on fretting fatigue, *International Journal of Fatigue*, 24 (2002) 763-775.

[6] Namjoshi, Mall, Jain and Jin, Effects of Process Variables on Fretting Fatigue Crack Initiation in Ti-6Al-4V, *The journal of Strain Analysis for Engineering Design*, 37 (6) (2002) 535-547.

[7] Walker K, The effect of stress ration during crack propagation and fatigue for 2024-T3 and 7075-T6 Aluminum Effects of Environment and Complex Load History on Fatigue life, *American Society for Testing and Materials*, (1970) 1-14.

[8] C. D. Lykins, S. Mall and V. K. Jain, Combined experimental-numerical investigation of fretting fatigue crack initiation, *International Journal of Fatigue*, 23 (2001) 703-711.

[9] K. Chan, Y. Lee, *Ruiz Program*, South West Research Institute, Personal Communication, (1998).

Ki Su Shin graduated Korea Air force Academy with a B.S. in Mechanical Engineering in March 1988. He then received his M.S. and Ph.D. degrees from Wichita State University in 1995, United States Air Force Institute of Technology in 2004, respectively. Dr. Shin is currently a Professor at the National Defense University in Seoul, Korea. His research interests include weapon systems structural analysis, air-borne weapon's life estimation based on damage tolerance analysis.